Electronic Supplementary information

Low-cost and eco-friendly Br-doped $Cu_7Sn_3S_{10}$ thermoelectric compound with *zT* around unit

Tingting Deng, [abc] Pengfei Qiu,*[a] Tong Xing, [a], Zhengyang Zhou, [a] Tian-Ran Wei, [d] Dudi Ren, [a] Jie Xiao, [a] Xun Shi*[a] and Lidong Chen [abc]

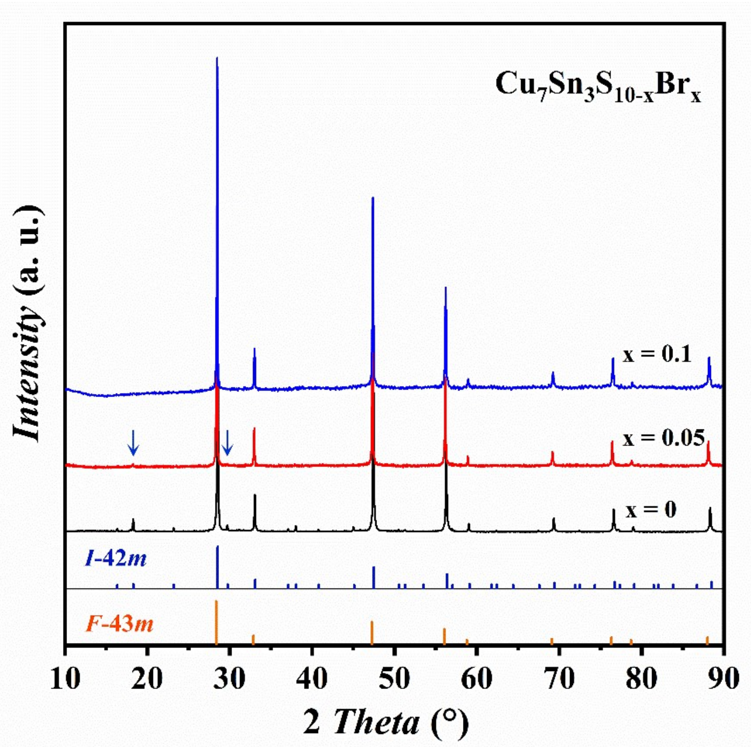

Fig. S1 Powder X-ray diffraction pattern (PXRD) of $Cu_7Sn_3S_{10-x}Br_x$ (x=0, 0.05, and 0.1) samples. The blue arrows represent the positions of the diffraction peaks for tetragonal phase.

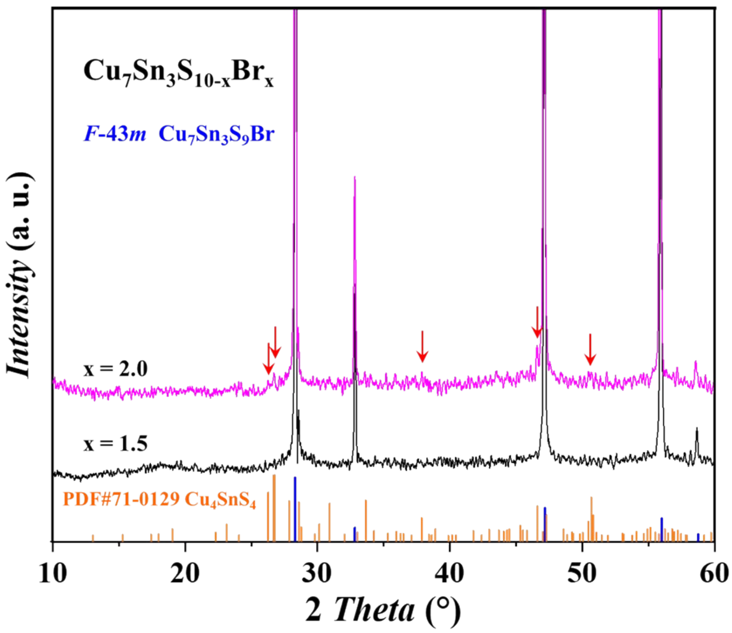

Fig. S2 Magnified powder X-ray diffraction pattern (PXRD) of $Cu_7Sn_3S_{10-x}Br_x$ (x=1.5 and 2.0) samples in the low intensity range. The red arrows represent the positions of the diffraction peaks for Cu_4SnS_4.

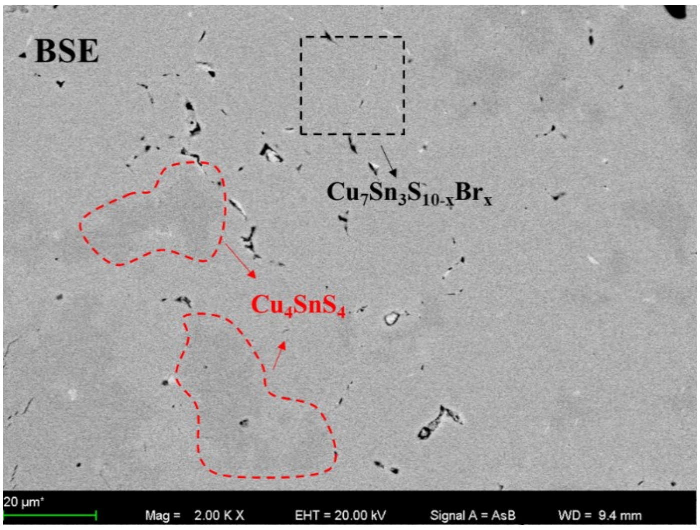

Fig. S3 Backscattered electron (BSE) image performed on $Cu_7Sn_3S_8Br_2$.

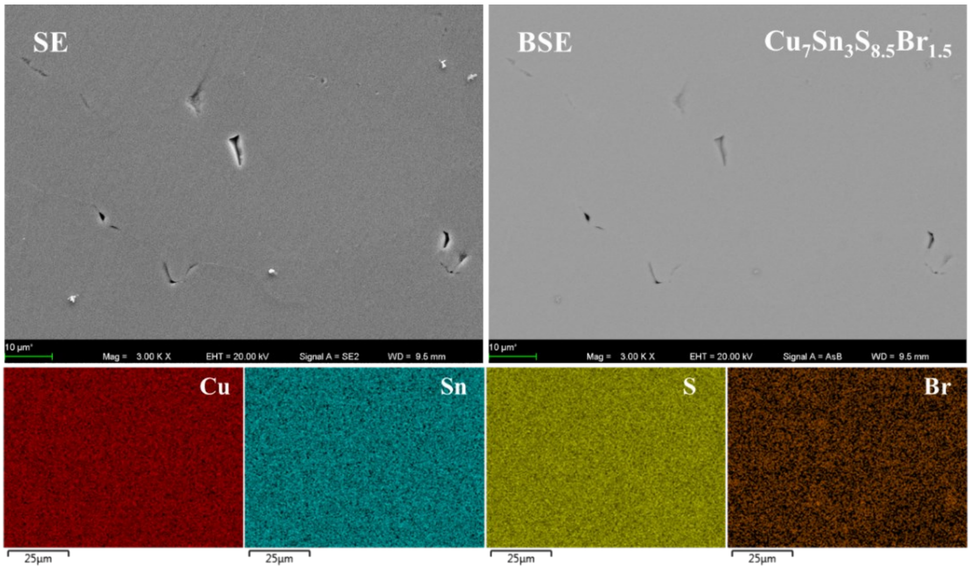

Fig. S4 Secondary electron (SE) image, Backscattered electron (BSE) image and Energy Dispersive X-ray Spectroscopy (EDS) mapping performed on $Cu_7Sn_3S_8Br_{1.5}$.

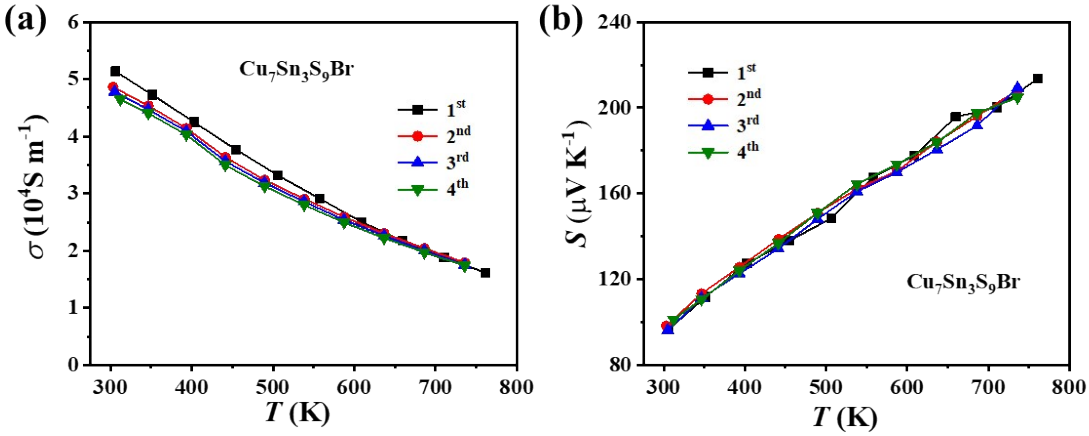

Fig. S5 Cycling test on electrical transport properties of $Cu_7Sn_3S_9Br$ sample.

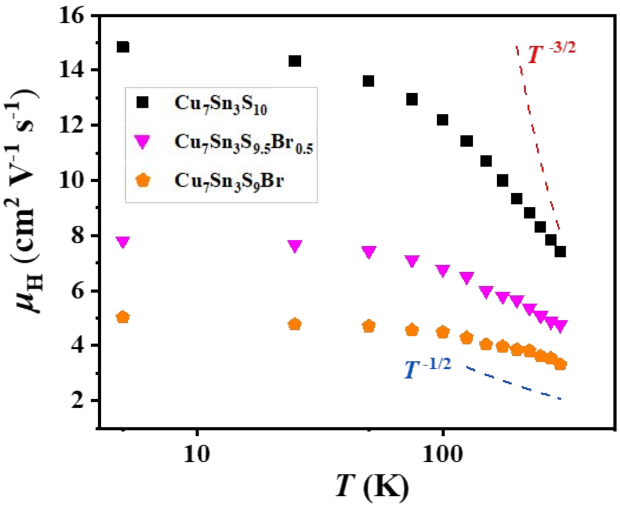

Fig. S6 Temperature dependence of Hall carrier mobility (μ_H) for $Cu_7Sn_3S_{10-x}Br_x$ (x=0, 0.5, and 1.0) samples from 5 K to 300 K. The dashed lines represent the acoustic phonon scattering (μ_H-$T^{-1.5}$) and alloy scattering (μ_H-$T^{-0.5}$), respectively.

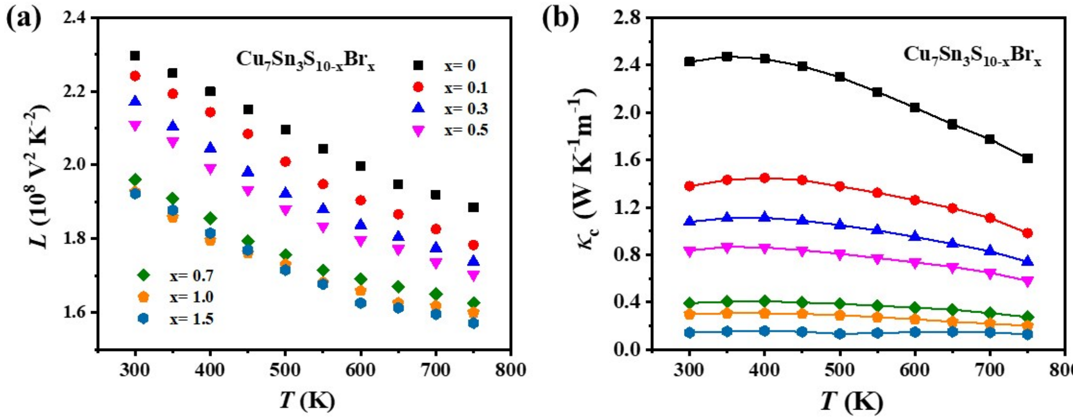

Fig. S7 Temperature dependences of (a) Lorenz number (L) and (b) carrier thermal conductivity (κ_c) for $Cu_7Sn_3S_{10-x}Br_x$ (x=0, 0.1, 0.3, 0.5, 0.7, 1.0, and 1.5).

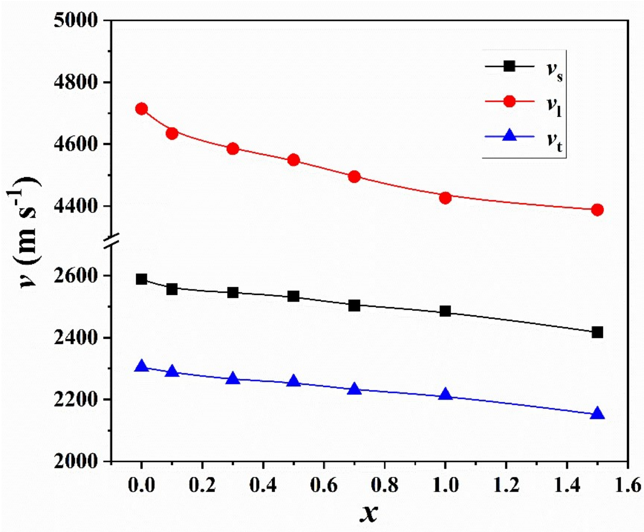

Fig. S8 Transverse sound velocity (v_t), longitudinal wave sound velocity (v_l), and average sound velocity (v_s) for Br-doped $Cu_7Sn_3S_{10}$ samples.

Table S1 Actual chemical compositions of the $Cu_7Sn_3S_{10-x}Br_x$ samples determined by EDS.

Nominal chemical compositions	Actual chemical compositions
$Cu_7Sn_3S_{10}$	$Cu_{6.51}Sn_3S_{9.89}$
$Cu_7Sn_3S_{9.9}Br_{0.1}$	$Cu_{6.62}Sn_3$ $S_{9.42}$ $Br_{0.11}$
$Cu_7Sn_3S_{9.7}Br_{0.3}$	$Cu_{6.68}Sn_3$ $S_{9.42}$ $Br_{0.28}$
$Cu_7Sn_3S_{9.5}Br_{0.5}$	$Cu_{6.72}Sn_3$ $S_{9.42}$ $Br_{0.38}$
$Cu_7Sn_3S_{9.3}Br_{0.7}$	$Cu_{6.59}Sn_3$ $S_{9.39}Br_{0.44}$
$Cu_7Sn_3S_9Br$	$Cu_{6.93}Sn_3$ $S_{9.22}Br_{0.46}$
$Cu_7Sn_3S_{8.5}Br_{1.5}$	$Cu_{6.49}Sn_3$ $S_{9.30}Br_{0.83}$
$Cu_7Sn_3S_8Br_2$	$Cu_{6.75}Sn_3$ $S_{8.96}Br_{0.63}$

Table S2 Atomic coordinates and isotropic displacement parameters for $Cu_7Sn_3S_9Br$.

Atom	Site	*x/a*	*y/b*	*z/c*	B_{eq} [Å^2]	Occupancy
Cu1	4*a*	0	0	0	1.24(10)	0.6999 Cu+0.3 Sn
S1	4*c*	1/4	1/4	1/4	0.7(2)	0.8999 S+0.1 Br

Table S3. Crystallographic information for $Cu_7Sn_3S_9Br$.

Composition	$Cu_{0.69}Sn_{0.3}S_{0.9}Br_{0.1}$
Formula weight	116.30
Space group	*F*3*m* (No. 216)
a /Å	5.4409(2)
Unit cell volume /$Å^3$	161.06(2)
F (000) /e	212.8
Z	4.0
μ/cm^{-1}	611.73
Calculated density (g cm^{-3})	4.8217(5)
Radiation, wavelength(Å)	Cu*K*α, 1.54056
T (K)	295
Data range 2θ (°)	5 – 100
No. of reflections	11
No. of refined structure parameters	7
Profile function	Pseudo-Voigt
Refinement mode	Full profile
R_i	0.0539
R_p	0.2932
R_{wp}	0.0857
Goodness of fit	13.140

Table S4 Selected Bond Lengths (Å) and Angles (°) for $Cu_7Sn_3S_9Br$.

Cu1-S1	**2.4014(1)**		
S1-Cu1-aS1	109.47(1)	Cu1-S1-aCu1	109.47(1)
S1-Cu1-bS1 [0000]	109.47(1)	Cu1-S1-bCu1 [0000]	109.47(1)
S1-Cu1-cS1 [0000]	109.47(1)	Cu1-S1-cCu1 [0000]	109.47(1)
aS1-Cu1-bS1 [0000]	109.47(1)	aCu1-S1-bCu1 [0000]	109.47(1)
aS1-Cu1-cS1	109.47(1)	aCu1-S1-cCu1	109.47(1)
bS1-Cu1-cS1	109.47(1)	bCu1-S1-cCu1	109.47(1)

Symmetry codes: +x, +y, +z; +z, +x, +y; +y, +z, +x; -y, +x, -z; -x, +z, -y; -z, +y, -x; +x, -y, -z; +z, -x, -y; +y, -z, -x; -y, -x, +z; -x, -z, +y; -z, -y, +x; -x, +y, -z; -z, +x, -y; -y, +z, -x; +y, +x, +z; +x, +z, +y; +z, +y, +x; -x, -y, +z; -z, -x, +y; -y -z, +x; +y, -x, -z; +x, -z, -y; +z, -y, -x;

Table S5 Density-of-state effective mass m_d^* for $Cu_7Sn_3S_{10-x}Br_x$ and $Cu_7Sn_3S_{10-x}Cl_x$ at

300 K and 750 K.

Compositions	m_d^*/m_e @300 K	m_d^*/m_e @750 K
$Cu_7Sn_3S_{10}$	3.5	4.2
$Cu_7Sn_3S_{9.9}Br_{0.1}$	4.0	4.9
$Cu_7Sn_3S_{9.7}Br_{0.3}$	4.0	4.8
$Cu_7Sn_3S_{9.5}Br_{0.5}$	4.1	4.8
$Cu_7Sn_3S_{9.7}Br_{0.3}$	4.6	5.3
$Cu_7Sn_3S_{9.0}Br_{1.0}$	4.7	5.9
$Cu_7Sn_3S_{8.5}Br_{1.5}$	4.6	6.8
$Cu_7Sn_3S_{9.7}Cl_{0.3}$	4.3	5.4
$Cu_7Sn_3S_{9.1}Cl_{0.9}$	5.4	7.1

Table S6 Detailed parameters used for the Callaway model. Here y (= x -0.1) is the normalized Br-doping content in $Cu_7Sn_3Br_{0.1}S_{9.9-y}Br_y$.

y	0	0.2	0.4	0.6	0.9	1.4
z(=y/9.9)	0	0.0202	0.0404	0.06061	0.09091	0.14141
1-z	1	0.9798	0.9596	0.93939	0.90909	0.85859
M_S	32.065	32.065	32.065	32.065	32.065	32.065
M_{Br}	79.904	79.904	79.904	79.904	79.904	79.904
r_S	1	1	1	1	1	1
r_{Br}	1.15	1.15	1.15	1.15	1.15	1.15
Γ_{mass}	0	0.00695	0.01339	0.01934	0.02738	0.03863
ε	--	635	635	635	635	635
Γ_{strain}	--	0.04706	0.09545	0.14493	0.22062	0.34871
Γ	--	0.05401	0.10884	0.16426	0.24801	0.38734
v_s (m s^{-1})	2556	2545	2533	2503	2485	2417
Θ_D (K)	280.9	279.7	278.5	275.1	273.2	265.7
u (300 K)	--	1.17472	1.67188	2.06579	2.54788	3.22849
u (500 K)	--	0.80962	1.15227	1.42375	1.75601	2.22508
u (750 K)	--	0.61603	0.87674	1.08331	1.33612	1.69303

Table S7 Fitting parameters used in theoretical zT prediction based on SPB model

T (K)	m_d^*/m_e	μ_0 (cm^2 V^{-1}s^{-1})	κ_L (W m^{-1} K^{-1})
300	4.0	17.0	1.4
	5.0	7.0	0.80
750	5.0	3.3	0.60
	6.0	1.5	0.40